A Multifaceted Mass Spectrometric Method to Probe Feeding Related Neuropeptide Changes in *Callinectes sapidus* and *Carcinus maenas*

Yuzhuo Zhang[1], **Kellen DeLaney**[2], **Limei Hui**[1], **Junhua Wang**[2], **Robert M. Sturm**[1], and **Lingjun Li**[1,2]

[1]School of Pharmacy, University of Wisconsin-Madison, 777 Highland Ave, Madison, WI 53705-2222, USA

[2]Department of Chemistry, University of Wisconsin-Madison, 1101 University Ave, Madison, WI 53706-1322, USA

Abstract

Food intake is regulated by various neuromodulators, including numerous neuropeptides. However, it remains elusive at the molecular and cellular level as to how these important chemicals regulate internal processes and which regions of the neuronal organs are responsible for regulating the behavior. Here we report a comparative neuropeptidomic analysis of the brain and pericardial organ (PO) in response to feeding in two well-studied crustacean physiology model organisms, *Callinectes sapidus* and *Carcinus maenas*, using mass spectrometry (MS) techniques. A multifaceted MS-based approach has been developed to obtain complementary information on the expression changes of a large array of neuropeptides in the brain and PO. The method employs stable isotope labeling of brain and PO extracts for relative MS quantitation, capillary electrophoresis (CE)-MS for fractionation and high-specificity analysis, and mass spectrometric imaging (MSI) for in-situ molecular mapping of peptides. A number of neuropeptides, including RFamides, B-type allatostatins (AST-B), RYamides, and orcokinins exhibit significant changes in abundance after feeding in this investigation. Peptides from the AST-B family found in PO tissue were shown to have both altered expression and localization changes after feeding, indicating that they may be a class of vital neuropeptide regulators involved in feeding behavior.
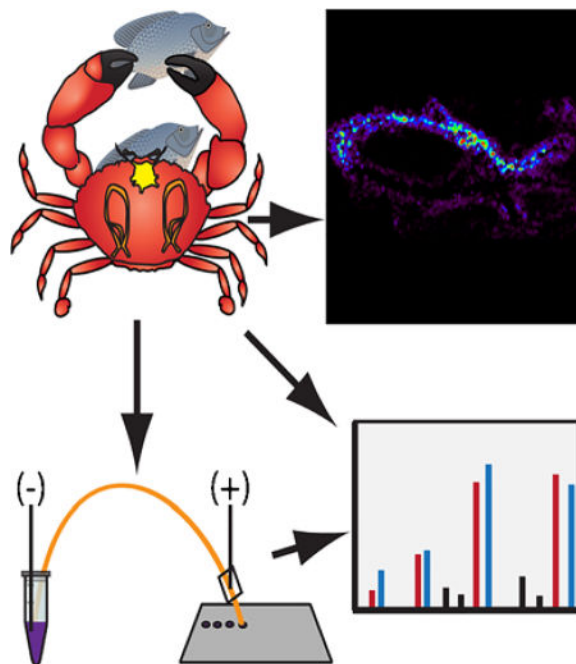
Graphical abstract

Keywords

Peptidomics; Neuropeptides; Isotopic labeling; Mass spectrometric imaging; Capillary electrophoresis

Introduction

The uptake of energy from the environment is essential to all organisms, as it is necessary for performing biological functions within the body. As organisms continuously consume energy to carry out functions necessary for survival, maintaining a reliable energy influx and functioning internal mechanisms for processing the energy are crucial to survival. In animals, the supply of energy comes from food intake, and, as such, its dysfunction may be correlated with diseases such as obesity, which in turn could lead to an increased risk of heart disease, diabetes, and stroke [1]. Food intake regulation utilizes an integrated response performed by neural circuits spanning from the central nervous system to peripheral signals, utilizing a wide variety of signaling molecules [2–4]. The complexity of this physiological process makes it difficult to study, and the identity and function of specific signaling molecules involved in the process remain elusive. Members of one of the most important and complex classes of signaling molecules, neuropeptides, have been shown to play a critical role in regulating the food intake process. Neuropeptides are short-chain amino acid sequences that function as neuromodulators or neurohormones and are essential to normal chemical signaling within the body. Recent efforts have focused on characterizing neuropeptides and their signaling pathways in a variety of species [5–9]. Furthermore, there have been numerous studies connecting specific neuropeptides with feeding behavior. For example, orexigenic neuropeptides galanin, neuropeptide Y (NPY), orexin, melanin-concentrating hormone, and corticotropin-releasing factor cause an increase in food intake,

whereas proopiomelanocortin, neurotensin, cholecystokinin (CCK), bombesin, tachykinin, and serotonin decrease food intake [1, 10–14]. However, the enormous technical challenges of studying the complex mammalian nervous system have prevented a more detailed understanding of the interplay between these neurotransmitters and hormones.

Invertebrate nervous systems are relatively simple and well-characterized. Consequently, they are used extensively to gain insights into the functional roles of endogenous peptides, especially neuropeptides, in food intake [15–19]. Invertebrate models are also highly relevant, as increasing evidence suggests that many of the signaling molecules and pathways underlying complex behaviors such as feeding are conserved across species. For example, the conserved NPY signaling pathway has been strongly implicated in the stimulation of food intake in vertebrates as well as in the regulation of the food-conditioned foraging behaviors of *Caenorhabditis elegans* [20, 21]. More recently, *Drosophila* neuropeptide F, a human NPY homologue, was reported to mediate food signaling through a conserved pathway [22]. Another neuropeptide family involved in the regulation of feeding behavior is composed of peptides terminating in Arg-Phe-NH$_2$, which belong to the RFamide family. A large number of RFamides have been characterized in invertebrates [23, 24], and members of the RFamide family have been demonstrated to be involved in feeding behavior in both vertebrates and invertebrates [25]. The conservation of peptide structure in the nervous systems of various animals and the previously demonstrated involvement of neuropeptides in feeding behavior enforce the validity of using invertebrate model systems for the identification of new regulatory peptides in feeding.

Callinectes sapidus, blue crab, and *Carcinus maenas*, green crab, were chosen as experimental models in this study because the neuropeptide complements of these two species have been extensively studied by immunohistochemistry [26–30] and mass spectrometry [31, 32]. Furthermore, the electrophysiology and anatomical connections of these systems are well-established [33–35]. The stomatogastric nervous system (STNS) neural network of crustaceans contains several central pattern-generating neural circuits that control the motion of gut and foregut. The STNS is composed of four ganglia, namely the stomatogastric ganglion (STG), esophageal ganglion (OG), and the paired commissural ganglia (CoG). The brain communicates with the STNS via the unpaired inferior ventricular nerve (*ivn*) and the paired circumesophageal commissures (*coc*) through CoGs [36]. The pericardial organs (POs), paired neurosecretory organs that surround the heart, function as major release sites of hormones and neuromodulators. By studying several key tissues in each species, we can gain insight into the overall mechanisms and signaling pathways involved in feeding behavior.

In this study, we employed stable isotope labeling to investigate the relative quantitative changes of diverse neuropeptide families in crustacean brains and pericardial organs (PO) between unfed and fed subjects. The results indicate the up-regulation of several neuropeptide families located in the crab brain after food intake, including tachykinins, orcokinins, and YRamides. Other families, such as RYamides, B-type allatostatins (AST-B), and RFamides, are significantly reduced in the PO. We also utilized matrix-assisted laser desorption/ ionization (MALDI)-MS imaging (MSI) to examine the distribution of neuropeptides of interest in the POs and observed neuropeptide localization changes induced

by feeding. Overall, this study further demonstrates that crustaceans provide useful model systems to study the neuroendocrine regulation of feeding, and that our multifaceted MS-based platform offers a powerful tool to directly examine neuropeptide expression changes under different physiological states.

Materials and Methods

Methanol, acetonitrile, formic acid, acetic acid, borane pyridine, and formaldehyde (FH_2) were purchased from Fisher Scientific (Pittsburgh, PA, USA). Deuterium formaldehyde (FD_2) was purchased from Isotech (Miamisburg, OH, USA). 2,5-Dihydroxybenzoic acid (DHB) was obtained from MP Biomedicals, Inc. (Solon, OH, USA). α-Cyano-4-hydroxycinnamic acid (CHCA) was purchased from Sigma-Aldrich (St. Louis, MO, USA). Acidified methanol was prepared using 90% methanol, 9% glacial acetic acid, and 1% water. All water used in this study was doubly distilled on a Millipore filtration system (Bedford, MA). C18 ziptips were purchased from Millipore (Billerica, MA, USA).

Animals and Feeding Experiments

Blue crabs *Callinectes sapidus* were purchased from a local grocery store, and green crabs *Carcinus maenas* were purchased from Marine Biological Lab (MA, USA). All animals were maintained without food in an artificial seawater tank at 12–13 °C for 5 d before use. In the feeding experiments, crabs were fed pieces of either fish or shrimp. The food was placed in the tank and the crabs were allowed to eat until they stopped, which usually took 45 min. Control crabs remained unfed prior to dissection. Crabs were then cold-anesthetized by being kept on ice for 15 min. Dissections were performed in chilled (approximately 10 °C) physiological saline (composition: 440 mM NaCl, 11 mM KCl, 13 mM $CaCl_2$, 26 mM $MgCl_2$, 10 mM trizmaHCl, pH 7.4 [adjusted with NaOH]). The details of dissection were described previously [37].

Tissue Extraction

To extract neuropeptides, the tissue samples were homogenized with a tissue homogenizer in 40 μL of acidified methanol (90/9/1 methanol/acetic acid/water). The homogenate was then transferred to a 1000 μL microcentrifuge tube. The solution was sonicated for 10 min to improve the extraction efficiency, and the resulting homogenate was centrifuged at 13,200 rpm for 10 min. The supernatant was transferred to another 1000 μL microcentrifuge tube and placed on ice. The tissue homogenizer was rinsed with 50 μL acidified methanol, and the resulting solution was used to wash the pellet in the microcentrifuge tube. The homogenate was centrifuged for 8 min and then added to the supernatant tube. The rinse and wash steps were repeated three times, and the combined supernatant was desiccated using a Savant SC 110 SpeedVac concentrator (Thermo Electron Corporation, West Palm Beach, FL, USA). The sample was then resuspended in 8 μL of Millipore water containing 0.1% formic acid (v/v). The crude extract was desalted using C18 ziptips according to the product instruction in order to remove lipids and salts before performing the formaldehyde labeling reaction.

In-Solution Formaldehyde Labeling

A 3 μL aliquot of tissue extract from brain or PO was labeled in solution by adding 0.7 μL borane pyridine (C_5H_8BN, 120 mM in 10% methanol) and mixing with formaldehyde (FH_2, 4% in H_2O, 0.5 μL) for unfed samples and deuterium formaldehyde (FD_2, 4% in H_2O, 0.5 μL) for fed samples. The samples were then left at room temperature for 15 min to allow the labeling reaction to go to completion. Aliquots of 4 μL from each solution were combined and mixed in a 1:1 ratio. The resulting mixture was spotted on a target plate and analyzed using MALDI-FTMS or MALDI-TOF/TOF.

Off-line CE-MALDI MS Analysis

Off-line CE separation was performed on a customized CE apparatus equipped with a capillary of 75 cm in length (50 μm i.d. × 360 μm o.d.). The CE runs were carried out with – 18 kV applied to the capillary inlet while the outlet was connected to ground. An ammonium formate buffer [50 mM, 2.5% MeOH (v/v) pH 3.5] was used and the runs were conducted at room temperature, 25 °C. The CE effluent was deposited every 60 s onto a MALDI target plate coated with parafilm with predeposited DHB matrix spots. The apparatus and procedure were described previously [26]. The collected CE effluents from 5 to 35 min were subsequently analyzed by MALDI-FTMS.

Mass Spectrometry and MALDI Imaging

MALDI-TOF/TOF—A model 4800 MALDI TOF/TOF MS analyzer (Applied Biosystems, Framingham, MA, USA) equipped with a 200 Hz, 355 nm Nd:YAG laser was used for brain and PO extract quantitation and MALDI imaging. For sample spotting, 0.4 μL of sample was spotted on the stainless steel MALDI plate first, allowed to dry, and followed by the addition of 0.4 μL of matrix solution. The matrix used was 5 mg/mL of α-cyano-4-hydroxycinnamic acid (CHCA) in 50% acetonitrile (v/v). Each sample was spotted twice onto the MALDI plate, and one spectrum was obtained for each pair of spots. Acquisitions were performed in positive ion reflectron mode. Instrument parameters were set using the 4000 Series Explorer software (Applied Biosystems). Mass spectra were obtained by averaging 900 laser shots covering a mass range of *m/z* 500 to 4000.

MALDI-FTMS

A Varian Fourier transform mass spectrometry (MALDI-FTMS) instrument (Lake Forest, CA) equipped with a 7.0 T actively-shielded superconducting magnet was used for CE separation analysis. All mass spectra were collected in the positive ion mode. The matrix was comprised of 150 mg/mL DHB in 50% MeOH (v/v). A 355 nm Nd:YAG laser (Laser Science, Inc., Franklin, MA, USA) was used to create ions that can be accumulated in the external hexapole storage trap before being transferred through a quadrupole ion guide to the ion cyclotron resonance (ICR) cell. The ions were excited prior to detection with an rf sweep beginning at 7050 ms with a width of 4 ms and amplitude of 150 V from base to peak. The filament and quadrupole trapping plates were initialized to 15 V, and both were ramped to 1 V from 6500 to 7000 ms to reduce baseline distortion of the peaks. Detection was performed in the broadband mode from *m/z* 108.00 to 2500.00.

MALDI Imaging

MALDI imaging of *C. sapidus* and *C. maenas* PO was performed as previously described [38]. Briefly, the PO was rinsed in water immediately following dissection to eliminate salt content. It was then positioned on a MALDI plate and placed in a desiccator to dry on the plate without being frozen or sectioned. Before imaging acquisition, five coats of DHB (150 mg/mL in 50% methanol, v/v) were applied on the tissue surface using an airbrush (Paasche Airbrush Company, Chicago, IL, USA) with 30 s of drying time between each coat. Imaging acquisition was performed on the model 4800 MALDI TOF/TOF analyzer (Applied Biosystems, Framingham, MA, USA) controlled using the 4800 Imaging application (Novartis, Basel, Switzerland) available through the MALDI MSI website (www.maldi-msi.org). To generate images, spectra were collected at 100 μm intervals in both the x and y dimensions across the surface of the sample. Each mass spectrum was generated by averaging 200 laser shots over the mass range *m/z* 800–2000. Individual spectra were acquired using 1.0 ns binning to yield 27812 data points per spectrum. Image files were then processed and extracted ion images were created using the TissueView software package (Applied Biosystems, Framingham, MA, USA).

Data Analysis of Quantitative Experiments

The spectra were analyzed manually using accurate-mass matching and the peak pairs corresponding to known crustacean neuropeptides were selected. The monoisotopic peak intensities of FH_2 (light)- and FD_2 (heavy)-labeled peak pairs were determined from these spectra. As the fed and unfed extracts for each replicate were run together in a single acquisition, the abundance ratio for each neuropeptide in fed crab versus unfed crab was determined by dividing the heavy-labeled peak intensity by the light-labeled peak intensity within the spectrum. Average ratios were calculated based on spectra from two duplicate experiments (technical replicates) in order to measure neuropeptide expression differences between the two samples in each acquisition. A Student's 2-tailed unequal variance test was also performed using Microsoft Excel in order to evaluate the differences between fed and unfed samples without assuming equal population variances. In the *t*-test, the intensities of FH_2- and FD_2- labeled peaks were normalized by dividing the intensity of each peak by the sum of the intensities of both peaks within the FH_2/FD_2-labeled peak pair to eliminate differences of ionization efficiency between different acquisitions (technical replicates).

Results and Discussion

This study sought to develop and implement an analytical method to characterize changes in neuropeptide regulation within the brain and PO of *C. sapidus* and *C. maenas*. Using stable isotope labeling with formaldehyde, we examined the quantitative changes of neuropeptide expression in fed animals versus unfed animals. As a control experiment, we examined isotopic formaldehyde labeled brain extracts from unfed animals showing approximately 1:1 ratio of light and heavy labeled peptide pairs with the same physiological state (Figure 1). To investigate the correlation between neuropeptide expression and localization, MALDI MS imaging was used to map the spatial distribution of several neuropeptides of interest in the PO. It has been shown that there is an observable and measurable change in both expression levels and localization patterns within the tissue for some neuropeptides, whereas others

remain unchanged. These findings provide insight into potential functions of these neuropeptides, indicating that certain neuropeptides participate to some extent in the regulation of feeding within crustaceans, whereas others do not appear to play a detectable role. As crustacean neuropeptides have numerous homologues in humans, this information may translate to the human neuropeptidome as well.

Quantitative Expression Changes of Neuropeptides in the Brain from Feeding

Quantitative changes in neuropeptide expression were examined in brains from four fed-unfed pairs of *C. maenas* and brains from five fed-unfed pairs of *C. sapidus*. Figure 1a shows a representative MALDI-TOF/TOF mass spectrum from one pair of brain extracts from *C. maenas*. The peak pairs of labeled neuropeptides are indicated with their corresponding masses. The abundance ratios (fed versus unfed) of several families of neuropeptides, including CabTRPs, orcokinins, RFamides, YRamides, and others, exhibited an increase. Table 1 lists the average abundance ratios from the four experiments for 18 neuropeptides detected in the *C. maenas* brain. Each ratio is calculated from two replicate MS spectra. The mean ratios averaged from the four groups of data and their corresponding *p*-values are also included. A representative MALDI-TOF/TOF mass spectrum comparing a pair of control animals is shown in Figure 1b. As can be seen, the ratios do not change appreciably between the control crabs, indicating that biovariability is not a substantial contributor to ratios deviating from unity in fed versus unfed animals. Therefore, it can be assumed that the ratios observed between fed and unfed animals represent changes due to feeding and not natural biovariability.

In *C. sapidus*, neuropeptides in the brain were relatively quantified in five groups of animals. Figure 2 shows a bar graph representation of abundance ratios (fed versus unfed) for 16 neuropeptides detected in the brain, including neuropeptides from the YRamide, CabTRP, RFamide, orcokinin, and SIFamide families. The y-axis represents the neuropeptide abundance ratios, and the x-axis provides the neuropeptide sequences. The error bars indicate standard error, and the corresponding *p*-values are displayed on the graph. Most of the neuropeptides showing significant differences suggest an increase in expression in the brain resulting from feeding, which is consistent with results found in previous studies on other species [39–43].

Significant changes ($p < 0.05$) are observed for members of several neuropeptide families, indicated by bold and italicized font in Table 1 for *C. maenas* and Figure 2 for *C. sapidus*. Of all of the neuropeptide families, YRamides are consistently increased by a relatively large amount in both species. In our previous study, YRamides showed elevation after food intake in *C. borealis* [39], and a similar trend was observed in *C. maenas* and *C. sapidus*. The YRamide HIGSLYRa (*m/z* 844.48) was increased by 1.5-fold in the fed *C. maenas* brain and by 1.6-fold in the *C. sapidus* brain. These results suggest that YRamides may have a function in brain processes associated with crustacean feeding regulation.

Members of the orcokinin family, one of the most abundant neuropeptide families present in crustacean brain, showed significant increases in fed *C. maenas* brain (approximately 1.2-fold, $p < 0.05$). This includes NFDEIDRSGFGFA (*m/z* 1474.63), NFDEIDRSGFGFV (*m/z* 1502.69), NFDEIDRSSFGFV (*m/z* 1532.70), and NFDEIDRSSFGFN (*m/z* 1547.68).

However, one of the isoforms detected, NFDEIDRSGFa (m/z 1198.55), did not show a consistent expression change ($p > 0.05$). Two isoforms from the orcokinin family, NFDEIDRSSFGFN (m/z 1547.68) and NFDEIDRTGFGFH (m/z 1554.70), showed higher expression levels after food intake in *C. sapidus*, whereas isoforms NFDEIDRSGFGFA (m/z 1474.63) and NFDEIDRSSFGFV (m/z 1532.70) did not change significantly. Orcokinin was first discovered by Stangier and colleagues in the crayfish *Orconectes limosus* and was reported to be a powerful stimulator of hindgut contractility [40]. A variety of other orcokinin isoforms were later discovered not only in decapods, but also in insects [41, 44–46]. In previous research, orcokinins were found to function as stimulators of gut muscles [40], as well as neuromodulators in crustaceans [41]. Interestingly, it was found that the same orcokinin isoform could have different functions in different species [47]. The quantitation data in this study shows that orcokinin isoforms increase in crab brain after eating, suggesting that orcokinins may also be involved in the regulation of feeding processes in crustaceans.

The RFamides are a neuropeptide family conserved in both invertebrate and vertebrate animal nervous systems. RFamides have long been known to regulate feeding as anorexigenic signaling molecules in mice [48], as well as in other animals [43]. Recent reports have shown that RFamides convert feeding motor programs from ingestive to egestive and depress feeding muscle contractions [42, 43]. Our study further confirms the anorexigenic functional roles of some RFamides involved in feeding in crustacean. Three RFamide isoforms, NRNFLRFa (m/z 965.54), DRNFLRFa (m/z 966.53), and APQGNFLRFa (m/z 1048.57), exhibited a small increase (approximately 1.15-fold) in the *C. maenas* brain after feeding, whereas the remaining RFamides did not consistently increase after food intake. Similarly, two RFamides, NRNFLRFa (m/z 965.54) and TNYGGFLRFa (m/z 1073.55) in *C. sapidus* showed a small elevation after feeding, whereas other RFamides, GLSRNYLRFa (m/z 1124.61), GYSKNYLRFa (m/z 1146.61), and YGNRSFLRFa (m/z 1158.62), did not change significantly.

Two neuropeptides from the CabTRP family, APSGFLGMRa (m/z 934.49), detected in both species, and TPSGFLGMRa (m/z 964.50) detectable in *C. maenas* only, showed significant increases after feeding. Other types of neuropeptides, such as SIFamide and proctolin, did not exhibit significant changes in either species' brain after feeding. In summary, multiple families of neuropeptides present in animal brains were studied by MS-based quantitation methods. Various neuropeptide families including CabTRPs, RFamides, YRamide, and orcokinins are likely involved in feeding regulation based on their changes in expression. This data suggests that food intake behavior is a complex process regulated by multiple signaling molecules, indicated by the variety of responses from the detected neuropeptides, and the brain plays a substantial role in such regulation.

Neuropeptide Release from the Pericardial Organs upon Feeding

The pericardial organ is an important neuroendocrine tissue and has long been known to be a major source of circulating hormones. Moreover, it has been shown that many of the hormones present in the PO can modulate the neural circuits in the STG [49]. Thus, it can be expected that this important neuroendocrine organ is involved in feeding regulation by

releasing neuropeptides and hormones into the hemolymph, or circulating fluid. Our previous research used *Cancer borealis* as an experimental model to test this hypothesis [39] and discovered that after food-intake, a variety of neuropeptide families were detected in the hemolymph, presumably released from the PO. To further correlate neuropeptide release with the feeding process, we performed a quantitative study of neuropeptides in the POs of fed and unfed *C. sapidus* and *C. maenas*. Figure 3 shows representative MALDI TOF/TOF mass spectra of four pairs of PO extracts from unfed and fed *C. maenas*. The details of the trends in neuropeptide expression changes in *C. maenas* are shown in Table 2. Figure 4 shows the abundance ratios of each detected neuropeptide in five pairs of PO extracts from unfed and fed *C. sapidus*. We were able to examine 18 neuropeptides from six families in *C. maenas* and 13 neuropeptides from five families in *C. sapidus*. In contrast to the quantitation data from the brain, most neuropeptides in the POs exhibited a reduction in expression levels after food intake, suggesting that feeding might trigger the release of these neuropeptides from the PO into the animal's hemolymph. This result is to be expected, as the PO is a prominent neurosecretory tissue that releases neuropeptides into the hemolymph to modulate the STG.

The RYamide family consists of neuropeptides with sequences highly conserved across different species. As described previously, RYamides have been found to be important to food-intake in various animals. Therefore, it is not surprising that these peptides are likely involved in the feeding process in crustaceans. All RYamides in *C. maenas* PO, FVGGSRYa (*m/z* 784.41), SGFYANRYa (*m/z* 976.46), and SSRFVGGSRYa (*m/z* 1114.47), and one RYamide in *C. sapidus* PO, SSRFVGGSRYa (*m/z* 1114.47), were found to decrease after feeding.

AST-B family members have been reported to exert physiological actions on the pyloric neural circuit in the stomach where they have inhibitory effects on the pyloric rhythm [50]. In this study, all of the detected AST-B family members showed a significant decrease after food intake in both species, with the exception of VPNDWAHFRGSWamide (*m/z* 1470.70). This further ties the role of AST-B neuropeptides to the feeding process. Neuropeptides from the AST-B family, including QWSSMRGAWa (*m/z* 1107.56), SGDWSSLRGAWa (*m/z* 1220.63), STNWSSLRSAWa (*m/z* 1293.65), and VPNDWAHFRGSWa (*m/z* 1470.74), exhibited reduced expression levels in *C. sapidus* PO extract. In *C. maenas*, the AST-B neuropeptides QWSSMRGAWa (*m/z* 1107.5) and STNWSSLRSAWa (*m/z* 1293.63) also showed reduced expression levels. However, the AST-B neuropeptide VPNDWAHFRGSWa (*m/z* 1470.7), which exists in most crustacean species, had a highly inconsistent response.

Other neuropeptides, including orcokinins NFDEIDRSGFGFV (*m/z* 1502.69) and NFDEIDRSSFGFV (*m/z* 1532.70) in *C. maenas*, and YRamide HIGSLYRa (*m/z* 844.48) and proctolin RYLPT (*m/z* 649.47) in *C. sapidus*, were reduced in the PO extracts of fed animals. The remaining detected neuropeptides did not exhibit significant changes.

CE Separation for Higher Peptidomic Coverage and Analytical Specificity

In blue crab *C. sapidus* brain, the AST-B family peptides were not detected, likely due to their abundance falling below the detection limit with direct MALDI-MS analysis. One possible reason is that the brain extracts are highly complex, containing numerous biological

molecules, such as lipids, protein fragments, and other endogenous peptides of high abundances. Another reason may be that the AST-B peptides are at lower abundances in *C. sapidus* compared with other species. To explore this, microscale separation utilizing CE was implemented in order to provide separation, effectively decreasing the complexity of the sample for MALDI-MS analysis. The low abundance AST-B isoforms, TSWGKFQGSWa (*m/z* 1182.57), TGWNKFQGSWa (*m/z* 1209.58), and GNWNKFQGSWa (*m/z* 1222.58), that were barely seen in direct MALDI TOF/TOF analysis are readily detected after CE separation (Supporting Information Supplementary Figures S1, S2, and S3). The TGWNKFQGSWa (labeled *m/z* 1237.61 and 1241.64) and GNWNKFQGSWa (labeled *m/z* 1250.61 and 1254.64) peak pairs indicate a small increase after food intake, while the pair of TSWGKFQGSWa (labeled *m/z* 1210.60 and 1214.63) did not exhibit this trend.

Feeding Regulation Associated with Neuropeptide Localization

Compared with traditional methods like immunohistochemistry, MALDI-MSI can be used to study the localization of multiple molecules simultaneously in a high throughput manner. MALDI-MSI has been applied to map many different types of molecules in tissues, including lipids, proteins, and peptides [51–54]. In this study, MALDI-MSI was used to examine the differential distribution of numerous neuropeptides in both fed and unfed *C. maenas* and *C. sapidus*. The structure of the POs in *C. sapidus* and *C. maenas* is similar to that of *C. borealis*, an already well-characterized species, as they contain a dorsal trunk, ventral trunk, anterior bar, and posterior bar. This is shown in Figure 5, which displays the optical images of the unfed and fed *C. sapidus* POs on a MALDI plate without matrix coating. Areas of the PO referenced are labeled on the optical images. A total of 20 neuropeptides from seven families were studied in *C. sapidus*, and 11 neuropeptides from five families were studied in *C. maenas* for location information, and example ion images for each unfed and fed pair are shown in Figures 5 and 6. In the quantitation study, AST-B, orcokinin, RYamide, and some RFamide peptides were found to have different expression levels after food intake in both species. Therefore, the localization of these neuropeptides was carefully examined in order to provide more information about neuropeptide secretion in relation to feeding. Figure 5 represents neuropeptide distribution in the POs of unfed and fed *C. sapidus*. Although RYamide and orcokinin families exhibit different expression levels after feeding behavior, the localizations of these two neuropeptide families remain unchanged in the dorsal trunk after feeding. Thus, it is possible that these neuropeptide families regulate feeding behavior by releasing neuropeptides into hemolymph but not through transport within tissue. Figure 6 shows the spatial distribution of neuropeptides in the POs from fed and unfed *C. maenas*. In unfed *C. maenas*, RYamides are present extensively in the entire PO. After feeding, they become more concentrated in the posterior bar region. Our group also conducted MS imaging experiments for *C. borealis* PO and found that RYamides were present in the anterior bar and adjacent nerves [38]. These observations suggest that the same isoforms can have different spatial distribution patterns in the tissue and are thus likely to play different roles in different species.

The results for MS imaging of *C. maenas* PO are shown in Figure 6. Figure 6i shows the optical images of the unfed and fed POs before matrix coating, with areas of the PO labeled. Figure 6ii.–vi. show the neuropeptide localization in unfed and fed *C. maenas* POs. AST-B

(Figure 6ii. and Supplementary Figure S5ii.–v.) is the most abundant neuropeptide family in the *C. maenas* PO. The AST-B neuropeptides QWSSMRGAWa (*m/z* 1107.52) (Figure 6ii.) and GSNWSNLRGAWa (*m/z* 1246.61) (Supplementary Figure S5v.) have especially high abundances in the PO of unfed *C. maenas* and are prevalent throughout the whole PO, following the distribution trend of the entire family. The presence of these AST-Bs decreases substantially after feeding, and they become more localized to the posterior and anterior bars. The RYamides (Figure 6iii. and Supplementary Figure S5vi.–viii.) are present throughout the unfed PO, with higher concentrations in trunk parts. However, these neuropeptides appear more localized to the posterior bar in the fed PO. The abundance of RFamides (Figure 6vi. and Supplementary Figure S5ix. and x.) and CCAP (Figure 6v. and Supplementary Figure S5xi.) in *C. maenas* PO is relatively low in both fed and unfed compared with other families but is higher in the posterior and anterior parts. The most interesting phenomenon is an expression level change for SIFamide (Figure 6vi. and Supplementary Figure S5xii.). Although this neuropeptide does not show a significant change in the extraction experiment, it exhibited much stronger signal after feeding in the imaging MS study.

Several example ion images for neuropeptides existing in both unfed and fed *C. sapidus* are shown in Figure 5ii.–viii., as well as Supplementary Figure S4, including 20 neuropeptides from seven families. In the unfed PO, all RYamides (Figure 5ii. and Supplementary Figure S4ii.–v.) are in half of the anterior bar and posterior bar whereas isoforms FVGGSRYa (*m/z* 784.41) and pEGFYSQRYa (*m/z* 1030.45) are also abundant in the dorsal trunk. In the fed PO, these same neuropeptides appear to be concentrated to primarily dorsal trunk. All AST-Bs (Figure 5iii. and Supplementary Figure S4vi.–ix.) in the unfed PO are present extensively in the entire anterior bar, whereas STNWSSLRSAWa (*m/z* 1293.65) is distributed throughout the whole PO tissue. In the fed PO, the neuropeptides appeared to be more distributed throughout the whole tissue, while still being more intense in the anterior bar. The CCAP PFCNAFTGCa (*m/z* 956.38) (Figure 5iv. and Supplementary Figure S4x.) is localized to the posterior bar of both the unfed and fed POs. The two AST-As shown (Figure 5v. and Supplementary Figure S4xi. and xii.) are present throughout the entire unfed PO tissue, but are most concentrated in the anterior bar. In the fed PO, these AST-As became more evenly distributed over the entire tissue. All detected RFamides (Figure 5vi. and Supplementary Figure S4xiii.–xvi.) are abundant in the anterior portion of both the unfed and fed POs. Orcokinin neuropeptides (Figure 5vii. and Supplementary Figure S4xvii.–xx.) share the similar distribution patterns among isoforms and are most concentrated in the dorsal trunk of both unfed and fed POs. Tachykinin APSGFLGMRG (*m/z* 992.50) (Figure 5 viii. and Supplementary Figure S4xxi.) is most abundant at the junction of the dorsal trunk and anterior part of the unfed PO and does not change substantially after feeding.

The AST-B neuropeptides exhibit consistent quantitative changes in expression level in both species, as evident by analyses of the PO extracts. Imaging studies reveal that this family also exhibits a change in localization after food intake in both species. As shown in Figure 5, all members of the AST-B family are prevalent in the anterior bar in unfed *C. sapidus* PO, while these isoforms become more widely distributed throughout the whole tissue after food intake. In *C. maenas*, AST-B isoforms are present extensively across the whole tissue, but

after feeding they are more concentrated in the posterior and anterior parts. This observation suggests potential regulatory roles of AST-B peptides in feeding behavior.

Tachykinin is a neuropeptide family conserved across many species, and a large number of studies have been conducted to characterize their various physiological functions [55–57]. Tachykinin has been reported to regulate food intake behavior in rats and goldfish [58–60] as well as feeding behavior in other animals [61–63]. It also has been found to affect olfactory and locomotive behavior in the fruit fly, *Drosophila melanogaster* [61–64]. The concentration of tachykinin is low in the PO tissue; therefore it is difficult to obtain accurate quantitation from extraction experiments. However, the imaging data reveals the distinct location of this peptide in the PO tissue of unfed and fed *C. sapidus*, which warrants further study to explore its functional role.

Conclusion

We employed isotopic formaldehyde labeling and MALDI MS-based methods to quantitatively study neuropeptide regulation of feeding behavior. Multiple neuropeptide families have been shown to be involved in the regulation of feeding behavior in both *C. sapidus* and *C. maenas*. MALDI-TOF/TOF imaging was utilized to map the spatial distribution of a multitude of neuropeptides from various peptide families. The combined isotopic labeling and mass spectrometric imaging analysis revealed that in addition to neuropeptide expression level changes after feeding, the locations of several neuropeptides also changed. For example, both the tissue expression level and distribution pattern of the AST-B family showed distinct changes in response to food intake. This multifaceted approach provides a list of potential neuropeptide candidates involved in feeding whose functional roles will be further investigated.

Supplementary Material

Refer to Web version on PubMed Central for supplementary material.

Acknowledgments

References

1. Hillebrand JJ, de Wied D, Adan RA. Neuropeptides, food intake, and body weight regulation: a hypothalamic focus. Peptides. 2002; 23:2283–2306. [PubMed: 12535710]

2. Schwartz MW, Woods SC, Porte D Jr, Seeley RJ, Baskin DG. Central nervous system control of food intake. Nature. 2000; 404:661–671. [PubMed: 10766253]

3. Lin X, Volkoff H, Narnaware Y, Bernier NJ, Peyon P, Peter RE. Brain regulation of feeding behavior and food intake in fish. Comp. Biochem. Physiol. A Mol. Integr. Physiol. 2000; 126:415–434. [PubMed: 10989336]

4. Gao Q, Horvath TL. Neurobiology of feeding and energy expenditure. Ann. Rev. Neurosci. 2007; 30:367–398. [PubMed: 17506645]

5. Podvin S, Bundey R, Toneff T, Ziegler M, Hook V. Profiles of secreted neuropeptides and catecholamines illustrate similarities and differences in response to stimulation by distinct secretagogues. Mol. Cell. Neurosci. 2015; 68:177–185. [PubMed: 26092702]

6. Hook V, Bandeira N. Neuropeptidomics mass spectrometry reveals signaling networks generated by distinct protease pathways in human systems. J. Am. Soc. Mass Spectrom. 2015; 26:1970–1980. [PubMed: 26483184]

7. Zhang XZ, Petruzziello F, Zani F, Fouillen L, Andren PE, Solinas G, Rainer G. High identification rates of endogenous neuropeptides from mouse brain. J. Proteome Res. 2012; 11:2819–2827. [PubMed: 22424378]

8. Goldsmith CJ, Städele C, Stein W. Optical imaging of neuronal activity and visualization of fine neural structures in non-desheathed nervous systems. PLoS One. 2014; 9(7):e103459. [PubMed: 25062029]

9. Daur N, Diehl F, Mader W, Stein W. The stomatogastric nervous system as a model for studying sensorimotor interactions in real-time closed-loop conditions. Front Comput. Neurosci. 2012; 6:13. [PubMed: 22435059]

10. Valassi E, Scacchi M, Cavagnini F. Neuroendocrine control of food intake. Nutrition, metabolism, and cardiovascular diseases. 2008; 18:158–168.

11. Jing J, Vilim FS, Horn CC, Alexeeva V, Hatcher NG, Sasaki K, Yashina I, Zhurov Y, Kupfermann I, Sweedler JV, Weiss KR. From hunger to satiety: reconfiguration of a feeding network by aplysia neuropeptide Y. J. Neurosci. 2007; 27:3490–3502. [PubMed: 17392465]

12. Volkoff H. The role of neuropeptide Y, orexins, cocaine, and amphetamine-related transcript, cholecystokinin, amylin and leptin in the regulation of feeding in fish. Comp. Biochem. Physiol. A Mol. Integr. Physiol. 2006; 144:325–331. [PubMed: 16326123]

13. Volkoff H, Canosa LF, Unniappan S, Cerda-Reverter JM, Bernier NJ, Kelly SP, Peter RE. Neuropeptides and the control of food intake in fish. Gen. Comp. Endocrinol. 2005; 142:3–19. [PubMed: 15862543]

14. Woods SC, Figlewicz DP, Madden L, Porte D Jr, Sipols AJ, Seeley RJ. NPY and food intake: discrepancies in the model. Regul. Pept. 1998; 75–76:403–408.

15. Kupfermann I, Weiss KR. Motor program selection in simple model systems. Curr. Opin. Neurobiol. 2001; 11:673–677. [PubMed: 11741016]

16. Sweedler JV, Li L, Rubakhin SS, Alexeeva V, Dembrow NC, Dowling O, Jing J, Weiss KR, Vilim FS. Identification and characterization of the feeding circuit-activating peptides, a novel neuropeptide family of aplysia. J. Neurosci. 2002; 22:7797–7808. [PubMed: 12196603]

17. Nusbaum MP, Beenhakker MP. A small-systems approach to motor pattern generation. Nature. 2002; 417:343–350. [PubMed: 12015615]

18. Marder E. Motor pattern generation. Curr. Opin. Neurobiol. 2000; 10:691–698. [PubMed: 11240277]

19. Fuzita FJ, Pinkse MW, Patane JS, Verhaert PD, Lopes AR. High throughput techniques to reveal the molecular physiology and evolution of digestion in spiders. BMC Genomics. 2016; 17:716. [PubMed: 27604083]

20. de Bono M, Bargmann CI. Natural variation in a neuropeptide Y receptor homolog modifies social behavior and food response in *C. elegans*. Cell. 1998; 94:679–689. [PubMed: 9741632]

21. Arora S. Anubhuti: Role of neuropeptides in appetite regulation and obesity–a review. NeuroPeptides. 2006; 40:375–401. [PubMed: 16935329]

22. Shen P, Cai HN. Drosophila neuropeptide F mediates integration of chemosensory stimulation and conditioning of the nervous system by food. J. Neurobiol. 2001; 47:16–25. [PubMed: 11257610]

23. Li C, Kim K, Nelson LS. FMRFamide-related neuropeptide gene family in *Caenorhabditis elegans*. Brain Res. 1999; 848:26–34. [PubMed: 10612695]

24. Taghert PH. FMRFamide neuropeptides and neuropeptide-associated enzymes in Drosophila. Microsc. Res. Tech. 1999; 45:80–95. [PubMed: 10332726]

25. Dockray GJ. The expanding family of -RFamide peptides and their effects on feeding behaviour. Exp. Physiol. 2004; 89:229–235. [PubMed: 15123557]

26. Chung JS, Zmora N. Functional studies of crustacean hyperglycemic hormones (CHHs) of the blue crab, *Callinectes sapidus* - the expression and release of CHH in eyestalk and pericardial organ in response to environmental stress. FEBS J. 2008; 275:693–704. [PubMed: 18190527]

27. De Martinez Gaspar Martins C, Bianchini A. Metallothionein-like proteins in the blue crab *Callinectes sapidus*: effect of water salinity and ions. Comp. Biochem. Physiol. A Mol. Integr. Physiol. 2009; 152(366–371)

28. Chung JS, Zmora N, Katayama H, Tsutsui N. Crustacean hyperglycemic hormone (CHH neuropeptides family: functions, titer, and binding to target tissues. Gen. Comp. Endocrinol. 2009; 166:447–454. [PubMed: 20026335]

29. Dillaman R, Hequembourg S, Gay M. Early pattern of calcification in the dorsal carapace of the blue crab, *Callinectes sapidus*. J. Morphol. 2005; 263:356–374. [PubMed: 15688443]

30. Brian JV, Fernandes T, Ladle RJ, Todd PA. Patterns of morphological and genetic variability in UK populations of the shore crab, *Carcinus maenas Linnaeus*, 1758 (Crustacea : Decapoda : Brachyura). J. Exp. Mar. Biol. Ecol. 2006; 329:47–54.

31. Ma MM, Bors EK, Dickinson ES, Kwiatkowski MA, Sousa GL, Henry RP, Smith CM, Towle DW, Christie AE, Li LJ. Characterization of the *Carcinus maenas* neuropeptidome by mass spectrometry and functional genomics. Gen. Comp. Endocr. 2009; 161:320–334. [PubMed: 19523386]

32. Wang J, Zhang Y, Xiang F, Zhang Z, Li L. Combining capillary electrophoresis matrix-assisted laser desorption/ionization mass spectrometry and stable isotopic labeling techniques for comparative crustacean peptidomics. J. Chromatogr. A. 2010; 1217:4463–4470. [PubMed: 20334868]

33. Saver MA, Wilkens JL, Syed NI. In situ and in vitro identification and characterization of cardiac ganglion neurons in the crab, *Carcinus maenas*. J. Neurophysiol. 1999; 81:2964–2976. [PubMed: 10368413]

34. Ma M, Szabo TM, Jia C, Marder E, Li L. Mass spectrometric characterization and physiological actions of novel crustacean C-type allatostatins. Peptides. 2009; 30:1660–1668. [PubMed: 19505516]

35. Schulz DJ, Goaillard JM, Marder EE. Quantitative expression profiling of identified neurons reveals cell-specific constraints on highly variable levels of gene expression. Proc. Natl. Acad. Sci. USA. 2007; 104:13187–13191. [PubMed: 17652510]

36. Kirby MS, Nusbaum MP. Central nervous system projections to and from the commissural ganglion of the crab *Cancer borealis*. Cell Tissue Res. 2007; 328:625–637. [PubMed: 17347812]

37. Kutz KK, Schmidt JJ, Li L. In situ tissue analysis of neuropeptides by MALDI FTMS in-cell accumulation. Anal. Chem. 2004; 76:5630–5640. [PubMed: 15456280]

38. DeKeyser SS, Kutz-Naber KK, Schmidt JJ, Barrett-Wilt GA, Li L. Imaging mass spectrometry of neuropeptides in decapod crustacean neuronal tissues. J. Proteome Res. 2007; 6:1782–1791. [PubMed: 17381149]

39. Chen R, Hui L, Cape SS, Wang J, Li L. Comparative neuropeptidomic analysis of food intake via a multi-faceted mass spectrometric approach. ACS Chem. Neurosci. 2010; 1:204–214. [PubMed: 20368756]

40. Stangier J, Hilbich C, Burdzik S, Keller R. Orcokinin: a novel myotropic peptide from the nervous system of the crayfish. *Orconectes limosus*. Peptides. 1992; 13:859–864. [PubMed: 1480511]

41. Li L, Pulver SR, Kelley WP, Thirumalai V, Sweedler JV, Marder E. Orcokinin peptides in developing and adult crustacean stomatogastric nervous systems and pericardial organs. J. Comp. Neurol. 2002; 444:227–244. [PubMed: 11840477]

42. Bechtold DA, Luckman SM. The role of RFamide peptides in feeding. J. Endocrinol. 2007; 192:3–15. [PubMed: 17210738]

43. Vilim FS, Sasaki K, Rybak J, Alexeeva V, Cropper EC, Jing J, Orekhova IV, Brezina V, Price D, Romanova EV, Rubakhin SS, Hatcher N, Sweedler JV, Weiss KR. Distinct mechanisms produce functionally complementary actions of neuropeptides that are structurally related but derived from different precursors. J. Neurosci. 2010; 30:131–147. [PubMed: 20053896]

44. Bungart D, Hilbich C, Dircksen H, Keller R. Occurrence of analogues of the myotropic neuropeptide orcokinin in the shore crab, *Carcinus maenas*: evidence for a novel neuropeptide family. Peptides. 1995; 16:67–72. [PubMed: 7716076]

45. Huybrechts J, Nusbaum MP, Bosch LV, Baggerman G, De Loof A, Schoofs L. Neuropeptidomic analysis of the brain and thoracic ganglion from the Jonah crab, *Cancer borealis*. Biochem. Biophys. Res. Commun. 2003; 308:535–544. [PubMed: 12914784]

46. Pascual N, Castresana J, Valero ML, Andreu D, Belles X. Orcokinins in insects and other invertebrates. Insect Biochem. Mol. Biol. 2004; 34:1141–1146. [PubMed: 15522610]

47. Dickinson PS, Stemmler EA, Barton EE, Cashman CR, Gardner NP, Rus S, Brennan HR, McClintock TS, Christie AE. Molecular, mass spectral, and physiological analyses of orcokinins and orcokinin precursor-related peptides in the lobster *Homarus americanus* and the crayfish *Procambarus clarkii*. Peptides. 2009; 30:297–317. [PubMed: 19007832]

48. Kavaliers M, Hirst M, Mathers A. Inhibitory influences of FMRFamide on morphine- and deprivation-induced feeding. Neuroendocrinology. 1985; 40:533–535. [PubMed: 4010892]

49. Li L, Kelley WP, Billimoria CP, Christie AE, Pulver SR, Sweedler JV, Marder E. Mass spectrometric investigation of the neuropeptide complement and release in the pericardial organs of the crab, *Cancer borealis*. J. Neurochem. 2003; 87:642–656. [PubMed: 14535947]

50. Fu Q, Tang LS, Marder E, Li L. Mass spectrometric characterization and physiological actions of VPNDWAHFRGSWamide, a novel B type allatostatin in the crab, *Cancer borealis*. J. Neurochem. 2007; 101:1099–1107. [PubMed: 17394556]

51. Hsieh Y, Chen J, Korfmacher WA. Mapping pharmaceuticals in tissues using MALDI imaging mass spectrometry. J. Pharmacol. Toxicol. Methods. 2007; 55:193–200. [PubMed: 16919485]

52. Cornett DS, Reyzer ML, Chaurand P, Caprioli RM. MALDI imaging mass spectrometry: molecular snapshots of biochemical systems. Nat. Methods. 2007; 4:828–833. [PubMed: 17901873]

53. Chaurand P, Norris JL, Cornett DS, Mobley JA, Caprioli RM. New developments in profiling and imaging of proteins from tissue sections by MALDI mass spectrometry. J. Proteome Res. 2006; 5:2889–2900. [PubMed: 17081040]

54. Shariatgorji M, Nilsson A, Goodwin RJA, Kallback P, Schintu N, Zhang XQ, Crossman AR, Bezard E, Svenningsson P, Andren PE. Direct targeted quantitative molecular imaging of neurotransmitters in brain tissue sections. Neuron. 2014; 84:697–707. [PubMed: 25453841]

55. Satake H, Kawada T, Nomoto K, Minakata H. Insight into tachykinin-related peptides, their receptors, and invertebrate tachykinins: a review. Zoolog. Sci. 2003; 20:533–549. [PubMed: 12777825]

56. Severini C, Improta G, Falconieri-Erspamer G, Salvadori S, Erspamer V. The tachykinin peptide family. Pharmacol. Rev. 2002; 54:285–322. [PubMed: 12037144]

57. Otsuka M, Yoshioka K. Neurotransmitter functions of mammalian tachykinins. Physiol Rev. 1993; 73:229–308. [PubMed: 7682720]

58. Kalra SP, Dube MG, Kalra PS. Neuropeptide K (NPK) suppresses copulatory behavior in male rats. Physiol. Behav. 1991; 49:1297–1300. [PubMed: 1896514]

59. Kalra SP, Sahu A, Dube G, Kalra PS. Effects of various tachykinins on pituitary LH secretion, feeding, and sexual behavior in the rat. Ann. NY Acad. Sci. 1991; 632:332–338. [PubMed: 1719876]

60. Peyon P, Saied H, Lin X, Peter RE. Preprotachykinin gene expression in goldfish brain: sexual, seasonal, and postprandial variations. Peptides. 2000; 21:225–231. [PubMed: 10764949]

61. Brockmann A, Annangudi SP, Richmond TA, Ament SA, Xie F, Southey BR, Rodriguez-Zas SR, Robinson GE, Sweedler JV. Quantitative peptidomics reveal brain peptide signatures of behavior. Proc. Natl. Acad. Sci. USA. 2009; 106:2383–2388. [PubMed: 19179284]

62. Pascual N, Maestro JL, Chiva C, Andreu D, Belles X. Identification of a tachykinin-related peptide with orexigenic properties in the German cockroach. Peptides. 2008; 29:386–392. [PubMed: 18178289]

63. Tachibana T, Khan MS, Matsuda K, Ueda H, Cline MA. Central administration of substance P inhibits feeding behavior in chicks. Horm. Behav. 2010; 57:203–208. [PubMed: 19909753]

64. Winther AM, Acebes A, Ferrus A. Tachykinin-related peptides modulate odor perception and locomotor activity in *Drosophila*. Mol. Cell Neurosci. 2006; 31:399–406. [PubMed: 16289899]
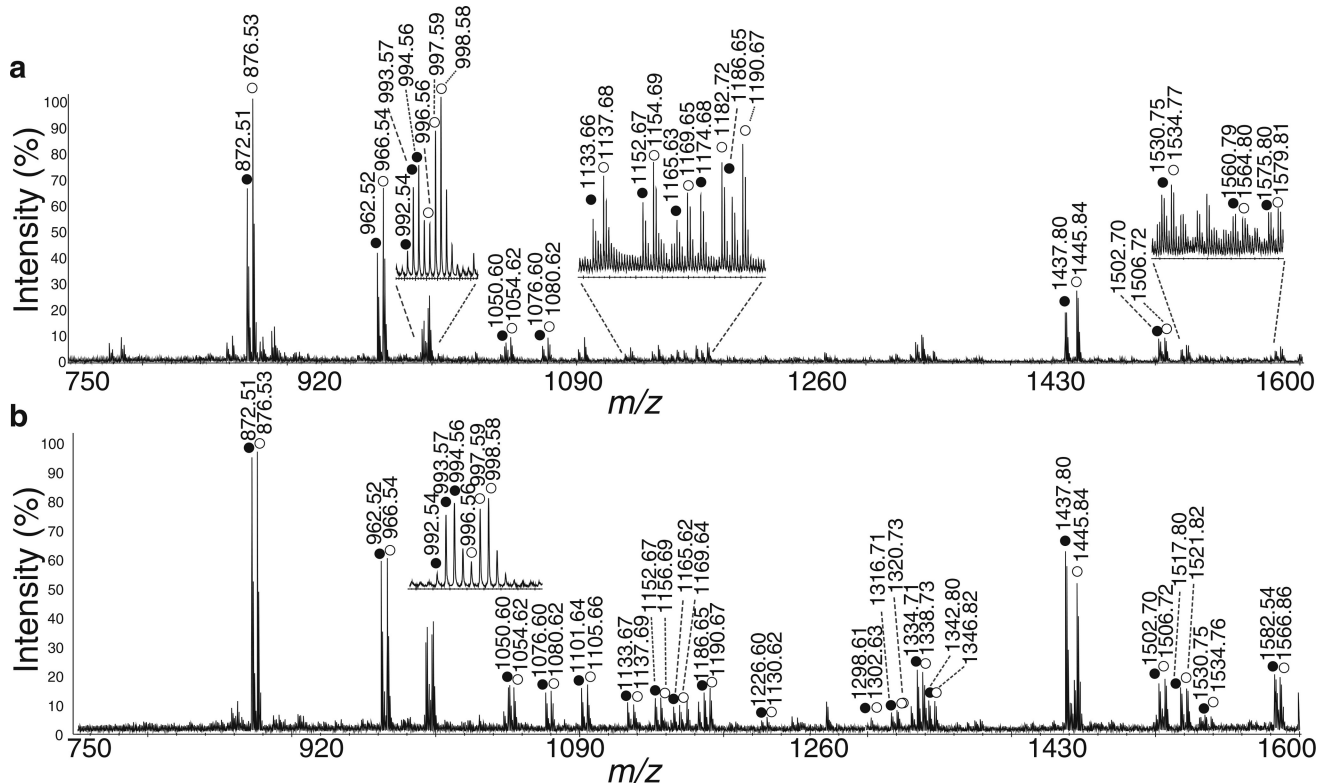
Figure 1.
(a) Representative MALDI-TOF/TOF spectrum of isotopic formaldehyde-labeled mixture of fed crab brain extract and unfed brain extract. Each extract was comprised of one unfed and one fed crab brain. Unfed sample was labeled with FH_2 and fed sample was labeled with FD_2. **(b)** Representative MALDI-TOF/TOF spectrum of formaldehyde labeled mixture of unfed crab brain extracts. Each extract was comprised of two unfed crab brains. One unfed sample was labeled with FH_2 and the other unfed sample was labeled with FD_2. The heavy labeled peaks are labeled with open circles, and the light labeled peaks are labeled with closed circles. The peak pairs from several abundant neuropeptides are indicated in each figure and annotated with their amino acid sequences
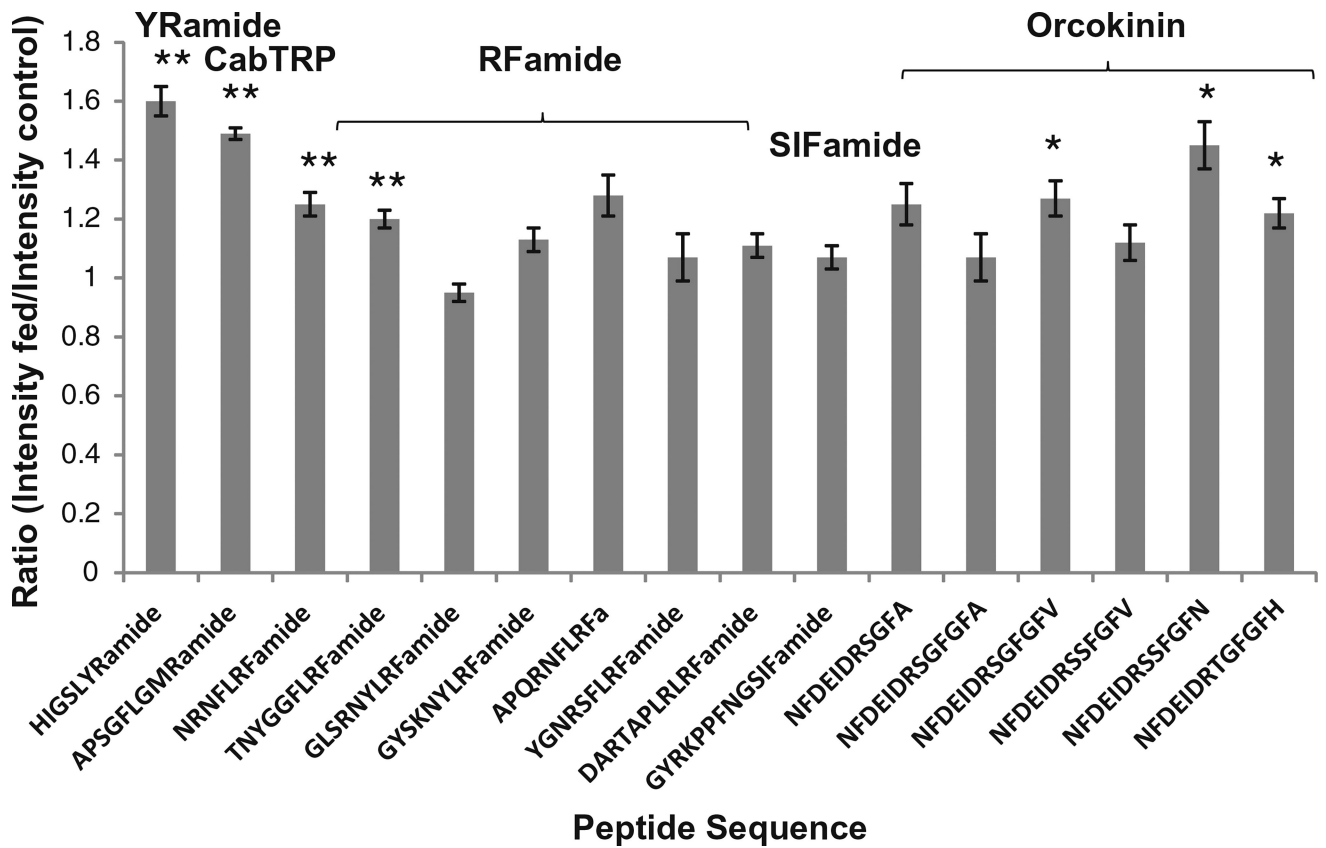
Figure 2.
Abundance ratios of 16 neuropeptides in *C. sapidus* fed brain versus unfed brain from five groups of feeding experiments. The sequence of each neuropeptide is labeled on the x-axis, and they are organized by families. The y-axis represents the abundance ratio of each neuropeptide between fed and unfed crab. * Indicates $p < 0.05$, ** indicates $p < 0.005$
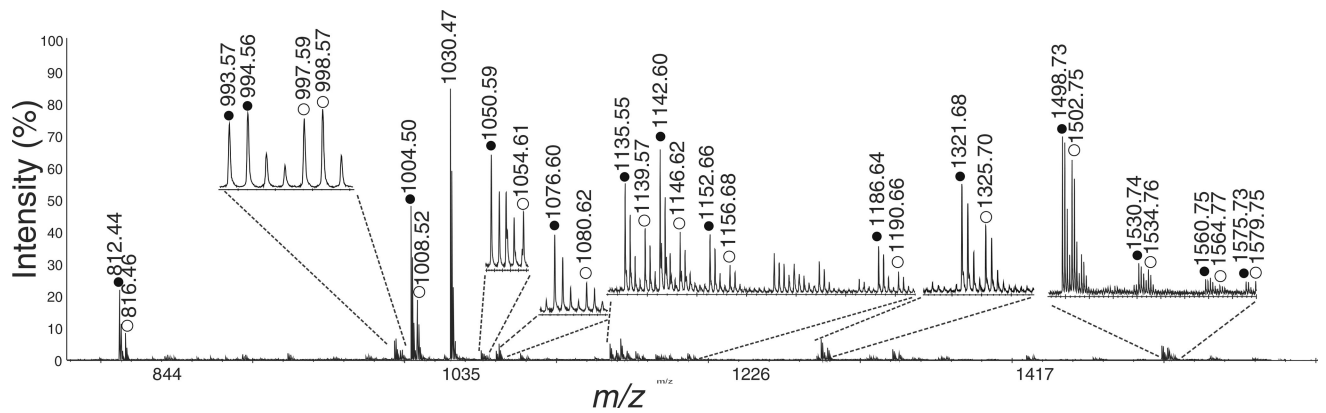
Figure 3.
Representative MALDI-TOF/TOF spectrum of a formaldehyde-labeled mixture of PO extract from fed and unfed *C. maenas*. Each extract was comprised of two POs from the same crab. Unfed sample was labeled with FH_2 and fed sample was labeled with FD_2. The heavy-labeled peaks are indicated with open circles, and the light-labeled peaks are indicated with closed circles. The peak pairs from several abundant neuropeptides are indicated and labeled with their amino acid sequences
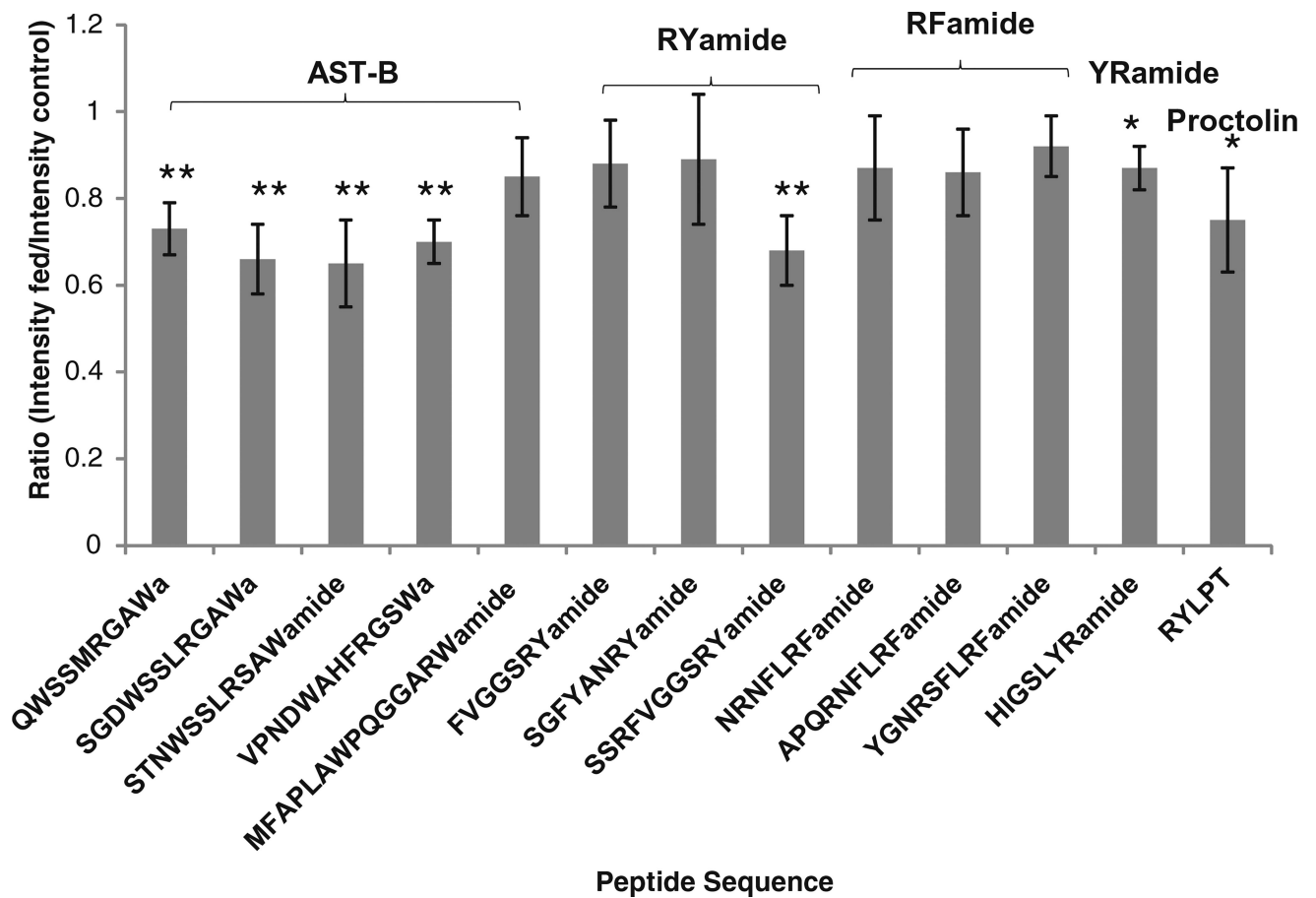
Figure 4.
Abundance ratios of 13 neuropeptides in the POs from fed *C. sapidus* versus unfed crabs
from five groups of feeding experiments. The sequence of each neuropeptide is labeled on
the x-axis, and they are organized in the order of families. The y-axis represents the
abundance ratio of each neuropeptide between fed and unfed crab. * Indicates $p < 0.05$, **
indicates $p < 0.005$ (n = 5)

Figure 5.
Neuropeptide localization in unfed and fed *C. sapidus* PO. (i.) Optical image of a PO tissue on a MALDI plate before being coated with DHB matrix. (ii. – xxi.) MALDI-MS images of several neuropeptides of interest from seven families: four RYamides, four AST-B peptides, one CCAP, two AST-A peptides, four RFamides, four orcokinins, and one tachykinin. The orientation of all the figures are the same

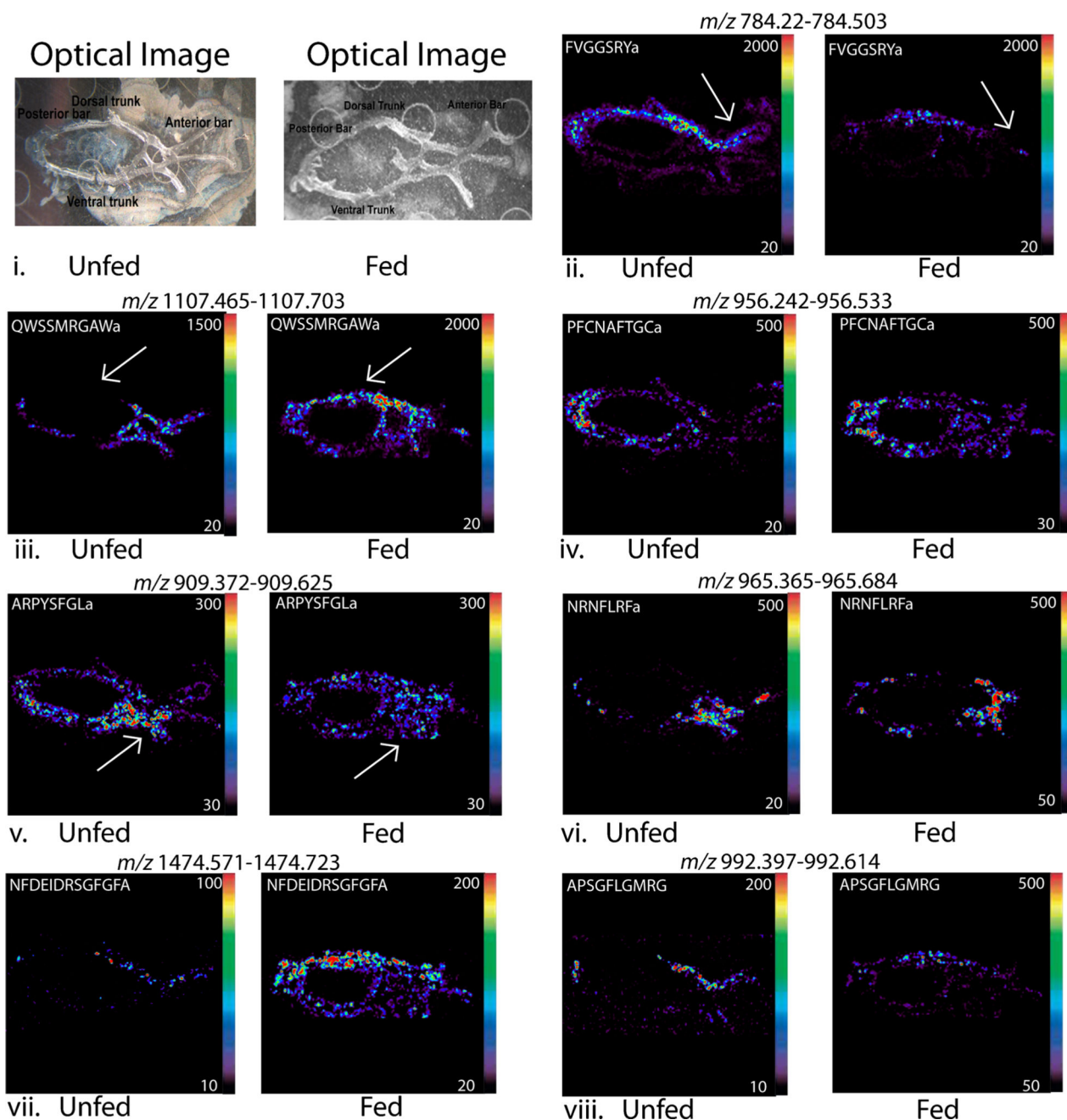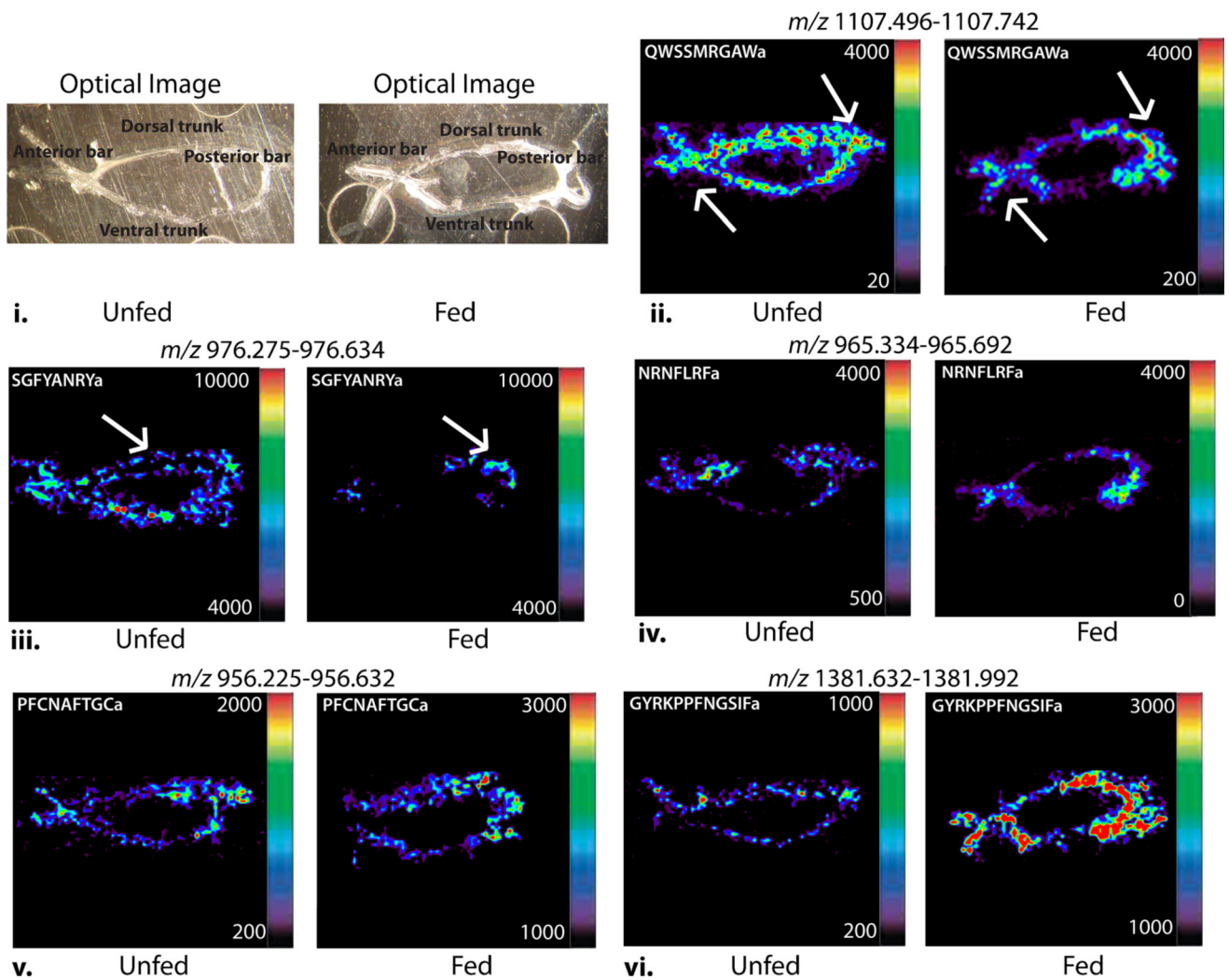**Figure 6.**
Neuropeptide localization in unfed and fed *C. maenas* PO. (i.) Optical image of a PO tissue on a MALDI plate before being coated with DHB matrix. (ii. – ix.) MALDI-MS images of several neuropeptides of interest from six families: including four AST-Bs, three RYamides, two RFamides, one CCAP, and one SIFamide. The orientation of all the figures are the same

Table 1

Ratios of Neuropeptide Expression in Fed and Unfed *Carcinus maenas* Brain from Four Groups of Feeding Experiments, the Average Ratios of Each Neuropeptide, and the Corresponding p-value[a]

Neuropeptide family	m/z	Sequence	Experiment				R average	p-value
			1	2	3	4		
RFamide	**965.54**	**NRNFLRFamide**	**1.05**	**1.18**	**1.14**	**1.25**	**1.15**	**0.033**
	966.53	**DRNFLRFamide**	**1.1**	**1.1**	**1.23**	**1.17**	**1.15**	**0.013**
	1022.57	GNRNFLRFamide	1.02	1.15	1.03	1.13	1.08	0.085
	1048.57	APQGNFLRFamie	1.22	1.04	1.19	1.26	1.18	0.031
	1105.63	SMPSLRLRFamide	1.02	1.02	1.27	1.17	1.12	0.054
	1124.63	GLSRNYLRFamide	1	1.12	1.22	1.13	1.12	0.083
	1137.59	DGNRNFLRFamide	1.2	1.09	1.26	1.03	1.15	0.058
	1158.62	YGNRSFLRFamide	1.01	1.05	1.05	1.29	1.1	0.2
Orcokinin	1198.55	NFDEIDRSGFamide	1.54	1.08	0.89	1.07	1.15	0.381
	1474.63	**NFDEIDRSGFGFA**	**1.66**	**1.41**	**1.26**	**1.15**	**1.37**	**0.029**
	1502.7	**NFDEIDRSGFGFV**	**1.13**	**1.18**	**1.27**	**1.24**	**1.2**	**0.006**
	1532.7	**NFDEIDRSSFGFV**	**1.19**	**1.18**	**1.1**	**1.13**	**1.15**	**0.004**
	1547.68	**NFDEIDRSSFGFN**	**1.2**	**1.15**	**1.05**	**1.11**	**1.13**	**0.024**
CabTRPs	**934.49**	**APSGFLGMRamide**	**1.45**	**1.26**	**1.25**	**1.29**	**1.31**	**0.004**
	964.5	**TPSGFLGMRamide**	**1.84**	**1.54**	**1.57**	**1.66**	**1.65**	**0.001**
Proctolin	649.37	RYLPT	0.94	1.07	1.24	1.26	1.13	0.195
YRamide	**844.48**	**HIGSLYRamide**	**1.33**	**1.74**	**1.44**	**1.37**	**1.47**	**0.008**
SIFamide	1381.74	GYRKPPFNGSIFamide	1.03	1.01	1.16	1.24	1.11	0.133

[a]Statistically significant ratios (*p*-value < 0.05) are indicated by bold and italicized font.

Table 2

Ratios of Neuropeptide Expression in Fed and Unfed *Carcinus maenas* Pericardial Organs (POs) from Four Groups of Feeding Experiments, the Average Ratio of Each Neuropeptide, and the Corresponding *p*-value[a]

Neuropeptide family	m/z	Sequence	Experiment				R_average	p-value
			1	2	3	4		
Protcolin	649.37	RYLPT	0.97	0.8	0.62	0.94	0.83	0.033
RYamide	*784.41*	*FVGGSRYamide*	*0.61*	*0.63*	*0.57*	*0.72*	*0.63*	*<0.001*
	976.46	*SGFYANRYamide*	*0.56*	*0.61*	*0.6*	*0.67*	*0.61*	*<0.001*
	1114.47	*SSRFVGGSRYa*	*0.57*	*0.7*	*0.63*	*0.65*	*0.64*	*<0.001*
RFamide	965.54	NRNFLRFamide	1.17	0.87	0.72	0.42	0.79	0.097
	966.53	DRNFLRFa	1.12	0.77	0.71	0.37	0.74	0.06
	1022.57	GNRNFLRFamide	1.19	0.87	0.87	0.41	0.84	0.136
	1048.57	*APQGNFLRFa*	*0.98*	*0.64*	*0.62*	*0.52*	*0.69*	*0.005*
	1124.63	*GLSPNYLRFa*	*0.57*	*0.79*	*0.7*	*0.38*	*0.61*	*0.003*
	1137.89	DGNRNFLRFa	1.31	1.06	0.88	0.73	1	0.773
	1158.62	YGNRSRLRFa	1.1	0.82	0.67	0.42	0.75	0.051
AST-B	*1107.58*	*QWSSMRGAWa*	*0.85*	*0.77*	*0.77*	*0.71*	*0.77*	*<0.001*
	1293.63	*STNWSSLRSAWamide*	*0.98*	*0.72*	*0.55*	*0.68*	*0.73*	*0.007*
	1470.7	VPNDWAHFRGSWamide	1.62	0.27	0.25	1.18	0.83	0.217
Orcokinin	*1502.69*	*NFDEIDRSGFGFV*	*0.91*	*0.92*	*0.76*	*0.82*	*0.85*	*0.003*
	1532.7	*NFDEIDRSSFGFV*	*0.7*	*0.77*	*0.65*	*0.62*	*0.68*	*<0.001*
	1547.68	NFDEIDRSSFGFN	0.86	1.1	0.89	0.65	0.88	0.1

[a] Statistically significant ratios (*p*-value < 0.05) are indicated by bold and italicized font.